N^{ε}-lysine acetylation determines dissociation from GAP junctions and lateralization of connexin 43 in normal and dystrophic heart

Claudia Colussi[a], Jessica Rosati[b], Stefania Straino[b], Francesco Spallotta[a], Roberta Berni[c], Donatella Stilli[c], Stefano Rossi[c], Ezio Musso[c], Emilio Macchi[c], Antonello Mai[d], Gianluca Sbardella[e], Sabrina Castellano[e], Cristina Chimenti[f], Andrea Frustaci[g], Angela Nebbioso[h], Lucia Altucci[h], Maurizio C. Capogrossi[b], and Carlo Gaetano[b,1]

[a]Laboratorio di Biologia Vascolare e Medicina Rigenerativa, Centro Cardiologico Monzino, 20138 Milan, Italy; [b]Laboratorio di Patologia Vascolare, Istituto Dermopatico dell'Immacolata, 00167 Rome, Italy; [c]Dipartimento di Biologia Evoluzionistica e Funzionale, Sezione di Fisiologia, Università di Parma, 43100 Parma, Italy; [d]Dipartimento di Chimica e Tecnologie del Farmaco, Istituto Pasteur-Fondazione Cenci Bolognetti, Università La Sapienza, 00185 Rome, Italy; [e]Dipartimento di Scienze Farmaceutiche, Università degli Studi di Salerno, 84084 Salerno, Italy; [f]Istituto San Raffaele La Pisana, Istituto di Ricovero e Cura a Carattere Scientifico, 00163 Rome, Italy; [g]Dipartimento di Scienze Cardiologiche, Respiratorie, Nefrologiche e Geriatriche, Università La Sapienza, 00161 Rome, Italy; and [h]Dipartimento di Patologia Generale, Seconda Università di Napoli, 80138 Naples, Italy

Edited* by Eric N. Olson, University of Texas Southwestern, Dallas, TX, and approved January 4, 2011 (received for review September 3, 2010)

Wanting to explore the epigenetic basis of Duchenne cardiomyopathy, we found that global histone acetylase activity was abnormally elevated and the acetylase P300/CBP-associated factor (PCAF) coimmunoprecipitated with connexin 43 (Cx43), which was N^{ε}-lysine acetylated and lateralized in mdx heart. This observation was paralleled by Cx43 dissociation from *N*-cadherin and zonula occludens 1, whereas pp60-c-Src association was unaltered. In vivo treatment of mdx with the pan-histone acetylase inhibitor anacardic acid significantly reduced Cx43 N^{ε}-lysine acetylation and restored its association to GAP junctions (GJs) at intercalated discs. Noteworthy, in normal as well as mdx mice, the class IIa histone deacetylases 4 and 5 constitutively colocalized with Cx43 either at GJs or in the lateralized compartments. The class I histone deacetylase 3 was also part of the complex. Treatment of normal controls with the histone deacetylase pan-inhibitor suberoylanilide hydroxamic acid (MC1568) or the class IIa-selective inhibitor 3-{4-[3-(3-fluorophenyl)-3-oxo-1-propen-1-yl]-1-methyl-1H-pyrrol-2-yl}-N-hydroxy-2-propenamide (MC1568) determined Cx43 hyperacetylation, dissociation from GJs, and distribution along the long axis of ventricular cardiomyocytes. Consistently, the histone acetylase activator pentadecylidenemalonate 1b (SPV106) hyperacetylated cardiac proteins, including Cx43, which assumed a lateralized position that partly reproduced the dystrophic phenotype. In the presence of suberoylanilide hydroxamic acid, cell to cell permeability was significantly diminished, which is in agreement with a Cx43 close conformation in the consequence of hyperacetylation. Additional experiments, performed with Cx43 acetylation mutants, revealed, for the acetylated form of the molecule, a significant reduction in plasma membrane localization and a tendency to nuclear accumulation. These results suggest that Cx43 N^{ε}-lysine acetylation may have physiopathological consequences for cell to cell coupling and cardiac function.

muscular dystrophy | protein acetylation

Duchenne muscular dystrophy (DMD) and Becker muscular dystrophy (BMD) represent important causes of inherited progressive dilated cardiomyopathy because of absence or reduction in amount or size of dystrophin. Although the alteration in dystrophin expression influences skeletal muscle regeneration and cardiac function with only partially overlapping mechanisms (1), the reduction of nitric oxide (NO) production and the presence of oxidative stress (OxS) (2) settles on common physiopathological features between the two muscular districts (3, 4). Both conditions, in fact, determine important epigenetic effects (5, 6) with potential developmental and functional consequences for skeletal and cardiac muscle. Specifically, NO was found to be relevant for the regulation of histone deacetylases (HDAC) (6), whereas the presence of OxS has been associated with increased acetylase (HAT) activity (7).

In the mdx mouse model of Duchenne dystrophinopathy, the deficient synthesis of NO is paralleled by abnormal OxS levels in skeletal muscle, heart, brain, and freshly isolated cells (8) (Fig. S1). Noteworthy, OxS has been recently implicated in the regulation of connexin 43 (Cx43) distribution and function in the heart (9, 10). Cardiac connexins are present in the GAP junctions (GJs) at the intercalated discs (ICDs), which physically delimitate cardiomyocytes. ICDs, in fact, are the membrane sites where individual cardiomyocytes are connected to each other. GJs, together with other cell to cell communication structures including adherent junctions (AJs) and desmosomes (Dms), are predominantly situated in the ICDs, where they ensure mechanical coupling between cells and enable propagation of electrical impulses throughout the heart. Cx43 is the most abundant connexin present in the heart; it is endowed with protein interaction domains and sites of posttranslation modification (PTM), where only phosphorylation and Cystein-S-nitrosylation (11) have been reported so far. Although Cx43 PTMs and protein–protein interactions, thought to be important for proper GJs formation localization and function, have been extensively investigated (12–14), the association with epigenetic enzymes and the presence of epigenetically controlled PTMs have not yet been reported. Intriguingly, evidence is accumulating that cell to cell junctions might initiate signals that modulate gene transcription and growth control through the nuclear localization of the Cx43 carboxyl-terminus fragment (15), a process that may, indeed, be regulated at the epigenetic level.

Our prior work described that mdx mice have an altered HDAC/HAT functional balance (8, 16, 17). Additional studies revealed that, in mdx heart, Cx43 is predominantly lateralized, a condition that correlates with the presence of oxidative stress (9) and alterations in the propagation of cardiac electrical impulses (18). A prolonged treatment (2–3 mo) with the HDAC inhibitor (DI) suberoylanilide hydroxamic acid (SAHA), which exerts a potent antiinflammatory action (19), normalized Cx43 localization, cardiomyocyte excitation, and impulse velocity (18), reducing the global level of histone acetylation (8). In light of this evidence, we were prompted to investigate whether Cx43 could be acetylated in

Author contributions: C. Colussi, G.S., M.C., and C.G. designed research; C. Colussi, J.R., S.S., F.S., R.B., S.R., E. Macchi, and A.N. performed research; A.M., G.S., S.C., C. Chimenti, and A.F. contributed new reagents/analytic tools; D.S., G.S., S.C., L.A., and C.G. analyzed data; and C. Colussi, E. Musso, M.C., and C.G. wrote the paper.

The authors declare no conflict of interest.

*This Direct Submission article had a prearranged editor.

[1]To whom correspondence should be addressed. E-mail: gaetano@idi.it.

This article contains supporting information online at www.pnas.org/lookup/suppl/doi:10.1073/pnas.1013124108/-/DCSupplemental.

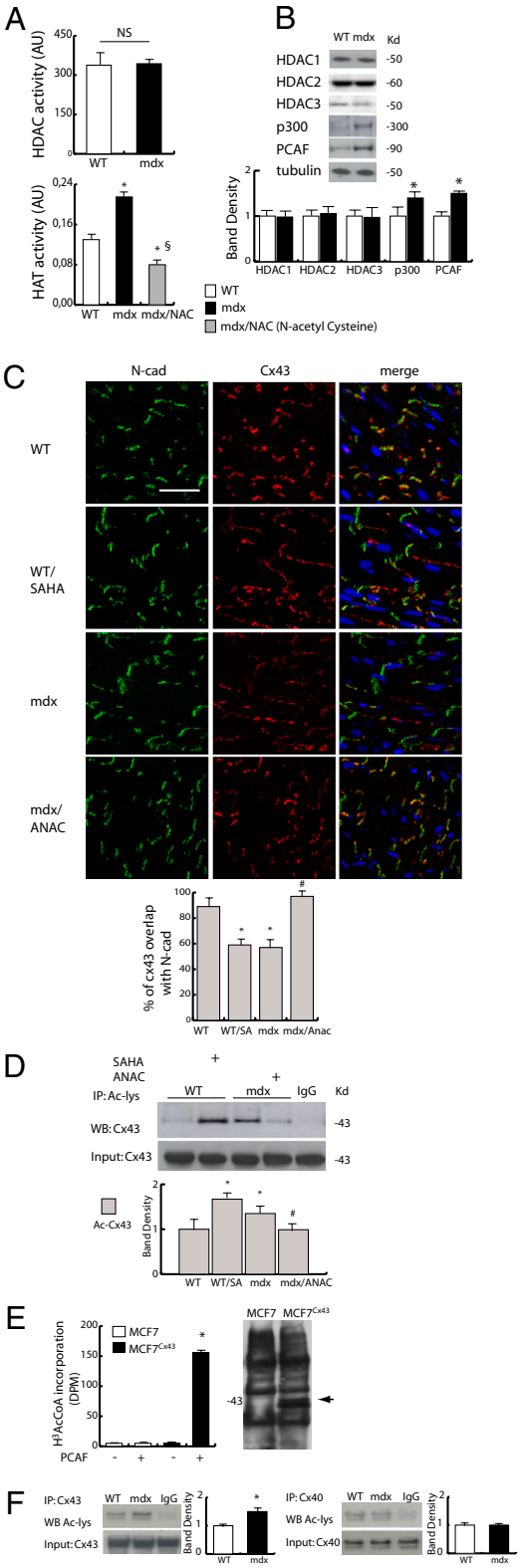

Fig. 1. Evaluation of epigenetic enzymes expression and Cx43 acetylation. (*A Upper*) Evaluation of HDACs activity in WT and mdx heart. (*Lower*) HAT activity in normal (WT), mdx, and mdx mice treated with *N*-acetyl cysteine (NAC). $^{*}P < 0.05$ vs. WT; $^{\S}P < 0.05$ vs. mdx. (*B*) Western blotting analysis of HDAC1, -2, and -3, p300, and PCAF expression in WT and mdx heart. Densitometry is shown in *Lower* ($P < 0.05$; $n = 3$). (*C Upper*) Confocal analysis of Cx43 (red) and *N*-cad (green) distribution in a heart section from WT, WT treated with SAHA, mdx, and mdx treated with anacardic acid (ANAC) mice. Nuclei were counterstained with 157199-63-8/Quinolinium, 4-{3-[3-methyl-2(3H)-benzothiazolylidene]-1-propenyl}-1-[3-(trimethylammonio)propyl]-,diiodide (TOPRO3) (blue). (Scale bar, 50 μm.) (*Lower*) The graph shows the degree of Cx43 and *N*-cad colocalization (%) at intercalated discs (ICDs). (*D*) Western blotting analysis of Cx43 acetylation level in WT, WT treated with SAHA, mdx, and mdx treated with ANAC mice. Densitometric analysis is shown in *Lower*. $^{*}P < 0.05$ vs. WT; $^{\#}P < 0.05$ vs. mdx. (*E*) H^3-acetyl-CoA in mock or cytomegalovirus promoter (pCMV)-Cx43–transfected MFC7 cells ($MCF7^{Cx43}$). Assays were performed in the presence or absence of recombinant PCAF added to the fresh lysate. *Right* shows Cx43 expression in mock and pCMV-Cx43 transfected MFC7 cells. (*F*) Immunoprecipitation and Western blotting analysis of Cx43 and connexin 40 (Cx40) expression and acetylation in the WT and mdx heart.

mdx and whether this specific PTM might have a role in Cx43 regulation and cell to cell communication. The following experimental points could be established: (*i*) N^{ε}-lysine acetylation of cardiac Cx43 occurs and determines its localization outside ICDs along the cardiomyocyte long axis, (*ii*) Cx43 associates with epigenetic molecules, including HATs and class I and IIa HDAC members, and (*iii*) epigenetic drugs able to enhance Cx43 N^{ε}-lysine acetylation alter Cx43 distribution in the normal heart, reduce cell to cell communication efficiency, and settle evidence in favor of an epigenetic control of cardiac function.

Results

Acetylated Form of Cx43 Delocalizes from GJs. Fig. 1*A* shows that total HAT activity is significantly increased in homogenates of mdx hearts compared with their normal controls, whereas that of HDACs is unaltered. This observation was paralleled by a relative increase in P300/CBP-associated factor (PCAF) and p300 expression but not class I HDACs, as indicated by Western blotting (Fig. 1*B*). Furthermore, the global acetylation of core histone H3 and tubulin was also increased (Fig. S2), suggesting that, in this physiopathological context, the level of HAT activity may have functional consequences on cardiac gene expression and protein function. The evidence that HAT function could be normalized by the in vivo treatment with the antioxidant *N*-acetyl-cystein (NAC) (20) provided a link to the endogenous OxS level as an upstream regulatory component of the signaling cascade leading to protein acetylation (Fig. 1*A*). In this condition, confocal microscopy revealed that Cx43, mostly lateralized in untreated mdx cardiomyocytes (18), returned to ICDs after treatment with the HAT pan-inhibitor anacardic acid (ANAC) (21) (Fig. 1*C*). On the contrary, a short-term treatment (96 h) of normal mice with SAHA, which increased total protein acetylation, determined dissociation of Cx43 from ICDs and lateralization, suggesting that Cx43 localization may be susceptible to regulation by the HDAC/HAT activity balance (Fig. 1*C*). Cx43 localization was further investigated in human heart samples obtained from dystrophic patients and found dissociated from ICDs compared with the normal human heart (Fig. S3). Whether the N^{ε}-lysine acetylation of Cx43 could be responsible of this phenomenon in humans remains to be ascertained.

Immunoprecipitation experiments confirmed that, in basal condition, the level of acetylated Cx43 was significantly higher in mdx than in normal controls (Fig. 1*D*). The intensity of this modification significantly increased in the heart of control animals treated for 96 h with SAHA, whereas it was counteracted in mdx exposed to ANAC (Fig. 1*D*). Further experiments confirmed that Cx43 can be acetylated in cell extracts exposed to radiolabeled Acetyl-CoA (H^3-ACoA) in the presence of a recombinant active acetylase (PCAF) (Fig. 1*E*).

In support of these findings, the recently available PHOSIDA website for N^{ε}-lysine acetylation prediction (www.phosida.org) (22) was used to analyze Cx43 protein sequence from different species. This analysis indicated the presence of at least three putative lysine N^{ε}-acetylation sites at positions 9 (K9), 234 (K234),

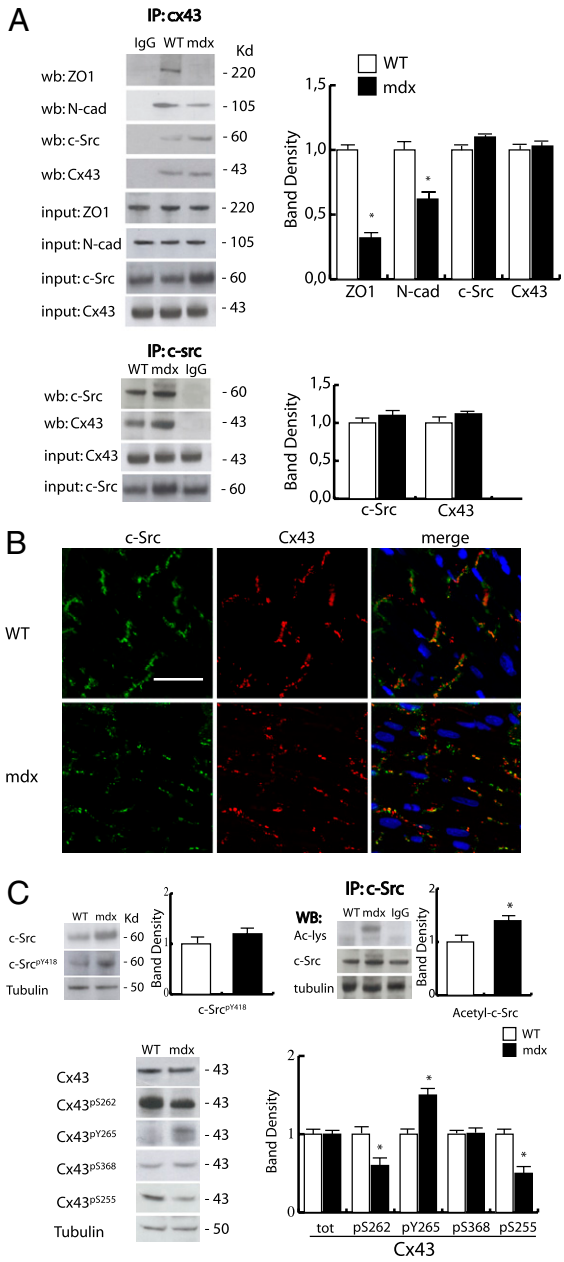

Fig. 2. Characterization of Cx43 phosphorylation and binding partners association. (*A Upper*) Immunoprecipitation analysis showing the association level of *N*-cad, ZO1, and c-Src with Cx43 in WT and mdx heart. (*Lower*) Association between c-Src and Cx43 in WT and mdx heart. Densitometric analyses are shown in *Right*. $*P < 0.05$. (*B*) Confocal analysis of c-Src (green) and Cx43 (red) distribution in WT and mdx heart. Nuclei were counterstained with TOPRO3 (blue). (Scale bar, 50 μm.) (*C*) Western blotting analysis showing phosphorylation level of c-Src (Y418) and Cx43 (S262, Y265, S368, and S255). *Right* shows band density. $*P < 0.05$.

and 264 (K264), which were conserved among species (*SI Appendix*). The acetylation of connexin 40, which does not present acetylation consensus sequences similar to Cx43, was found unaltered in mdx mice compared with normal controls (Fig. 1*F*).

Acetylated Cx43 Forms New Protein–Protein Interactions. In the normal heart, Cx43 is dynamically associated with multiple proteins, including the zonula occludens 1 (ZO1), cadherins (CAD), and pp60-cSrc (c-Src), and regulates conductivity through GJs (23, 24). In the dystrophic heart (Fig. 2*A*), although the association with ZO-1 and *N*-cadherin (*N*-CAD) diminished, the association between c-Src and the acetylated Cx43 was apparently stable and similar to that of controls. The association of c-Src with the lateralized form of Cx43 was further investigated by confocal microscopy (Fig. 2*B*). Although total c-Src levels increased in mdx, its phosphorylation on tyrosine 416 (Y416) did not change compared with controls (Fig. 2*C*). In this context, however, the phosphorylation of Cx43 at tyrosine 265 (Y265), one of the c-Src substrates, was significantly increased and paralleled by a reduction of signal from serine 262 (S262) and 255 (S255), respectively targets of $p34^{CDC2}$ and MAPK, whereas no changes in serine 368 recognized by protein kinase A\PKC kinases were detected (12) (Fig. 2*C Left*). The increase of c-Src expression in mdx heart is currently unexplained. A series of immunoprecipitation experiments, however, revealed a degree of N^{ε}-lysine acetylation for this molecule as well (Fig. 2*C Right*). Although it will require further investigations to determine the role of this specific PTM on c-Src, it may be conceivable that N^{ε}-lysine acetylation could affect c-Src turnover or function (25), influencing Cx43 phosphorylation in mdx. Intriguingly, c-Abl, another c-Src family member, has been previously reported as acetylated on lysine, with important consequences on its intracellular localization and function (26).

Histone Acetylase PCAF Is Involved in Cx43 Acetylation. To establish which acetylase is involved in the regulation of Cx43, a series of confocal and coimmunoprecipitation experiments were performed in normal and mdx mice. Fig. 3 *A* and *B* shows that PCAF, up-regulated in mdx cardiomyocytes (Fig. 1*B*) and distributed along sarcomeres (27), coimmunoprecipitated with Cx43, suggesting that it could be considered an acetylase associated with the connexin (Fig. 3*B*). To further investigate the role of PCAF in the acetylation of Cx43, a series of experiments were performed in normal control mice treated with the PCAF activator SPV106 (28). Fig. 3*C* shows that, in the presence of SPV106, Cx43 (administered daily for 4 d) dissociated from GJs, assuming a predominantly lateralized localization where its acetylation levels were increased (Fig. 3*D*).

Acetylated Cx43 Shows Cytoplasm and Nuclear Localization in Transfected National Institutes of Health (NIH) 3T3 Fibroblasts and Dystrophic Hearts. To assess the relevance of N^{ε}-lysine acetylation in Cx43 intracellular distribution, a series of mutants were generated bearing substitution of lysines at position 9, 234, and 264, with an equivalent number of acetyl-mimetic glutamine (Q) or the nonacetylatable alanine (A) defining the $Cx43^{(3Q)}$ and $Cx43^{(3A)}$ mutant forms of the molecule. Transient transfections were performed in recipient NIH 3T3 cells, which express low Cx43 basal protein levels compared with cells of cardiac origin (Fig. 4*A a*, *a Inset*, *b*, and *b Inset* and Fig. S4*A Left*). Fig. 4*A* shows that WT Cx43 [$Cx43^{(WT)}$] and the $Cx43^{(3A)}$ mutant were localized on the plasma membrane at cell to cell junctions (Fig. 4 *A c*, *c Inset*, *e*, and *e Inset* and *B Left*), whereas the $Cx43^{(3Q)}$ mutant was predominantly confined in the cytoplasm and at least in part, in the nucleus (Fig. 4 *A g* and *g Inset* and *B Right*). Consistently, in the presence of the pan-HDACi trichostatin A (TSA), which increases total intracellular protein acetylation, $Cx43^{(WT)}$ reduced its presence at cell to cell junctions, increasing its cytoplasmic and nuclear localization (Fig. 4 *Ad* and *B Left* and *Right*). TSA treatment did not influence Cx43 localization of $Cx43^{(3A)}$ and $Cx43^{(3Q)}$ mutants (Fig. 4 *A f* and *h* and *B Left* and *Right*). Noteworthy, in mdx heart, confocal, and Western blotting analyses revealed a cytosolic and nuclear distribution of Cx43 similar to that of $Cx43^{(3Q)}$ mutant (Fig. S4 *B* and *C*), further supporting the evidence that acetylation may influence Cx43 intracellular distribution. Functionally, the presence of acetylated Cx43 reduced about 70% cell to cell diffusion of the vital dye Calcein-AM in cells of cardiac origin (HL-1) (Fig. S5),

CELL BIOLOGY

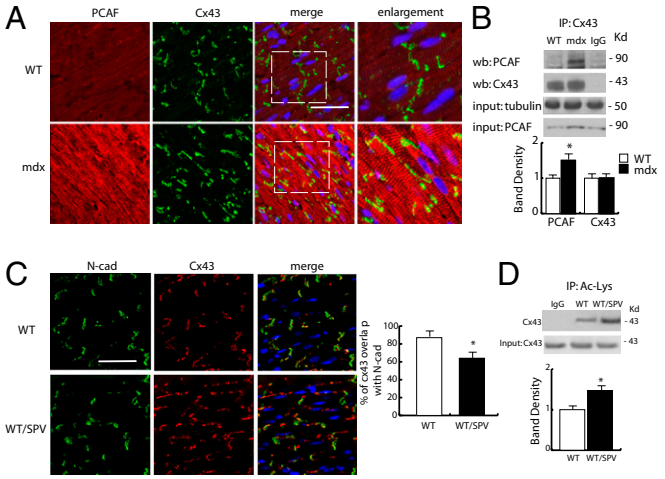

Fig. 3. Evaluation of PCAF distribution and function. (*A*) Panels show representative confocal images depicting PCAF (red) and Cx43 (green) expression and distribution in WT and mdx heart. Nuclei were counterstained with TOPRO3 (blue). (Scale bar, 50 μm.) The far right column shows enlarged details identified by brackets. (Scale bar, 50 μm.) (*B Upper*) Coimmunoprecipitation analysis of PCAF and Cx43 in the mdx heart. (*Lower*) Densitometric analysis. $*P < 0.05$. (*C*) Confocal analysis of *N*-cad (green) and Cx43 (red) distribution from control and SPV106-treated WT mice hearts. Nuclei were counterstained with TOPRO3 (blue). (Scale bar, 50 μm.) *Right* shows percentage of Cx43 and *N*-cad overlapping at ICDs level. (*D*) Immunoprecipitation experiment showing increase in Cx43 acetylation in WT treated with SPV106 or equivalent amount of solvent. Densitometric analysis is shown on the right. $*P < 0.05$.

showing a role for Cx43 acetylation in the negative regulation of intercellular signal transmission.

Class I and IIa Histone Deacetylases Form Complexes with Cx43. Prior data indicated that PCAF and class IIa HDAC4 colocalized to cardiac sarcomeres, contributing to the regulation of cardiomyocyte contractility (27). To investigate whether HDACs could be involved in the regulation of Cx43 acetylation, the localization and association of HDAC2, -3, -4, -5, -6, and -9 to Cx43 were examined. Fig. S6*A* shows that HDAC2 was equally expressed and localized to the nucleus in both normal and dystrophic mice, whereas HDAC9 was cytoplasmic and mostly localized to sarcomeres (Fig. S6*B*). HDAC6 was mostly nuclear in mdx and cytoplasmic in control animals (Fig. S6*C*). Surprisingly, HDAC3, -4, and -5, known to associate with each other to form dynamic complexes (29), colocalized with Cx43 in dystrophic and normal cardiomyocytes, although in the latter, HDAC3 was detectable to a lesser extent (Fig. 5 *A* and *B*). Specifically, these HDACs colocalized with Cx43 either when it was properly associated with GJs at the ICDs or when it was in lateralized position (Fig. 5*A*). The association of Cx43 with HDAC4 and -5 was also observed in the cardiac-derived transformed cell line HL-1 (Fig. S7). This phenomenon was further confirmed by coimmunoprecipitation experiments, which showed a constitutive association of HDAC3, -4, and -5 with Cx43 in normal and mdx total heart extracts (Fig. 5*B*). To functionally probe the role of class II HDACs, we measured the specific activity of HDAC4 and found that it was slightly but significantly decreased in mdx heart (Fig. 5*C*). Consistently, when normal mice were treated with the class IIa-specific inhibitor 3-{4-[3-(3-fluorophenyl)-3-oxo-1-propen-1-yl]-1-methyl-1H-pyrrol-2-yl}-N-hydroxy-2-propenamide (MC1568) (30), Cx43 dissociated from GJs, assuming a lateralized distribution (Fig. 5*D*); this suggests that, in normal conditions, class II HDACs may have a role in stabilizing Cx43 localization to GJs or ICDs. Taken altogether, these results indicate that combinatorial complexes

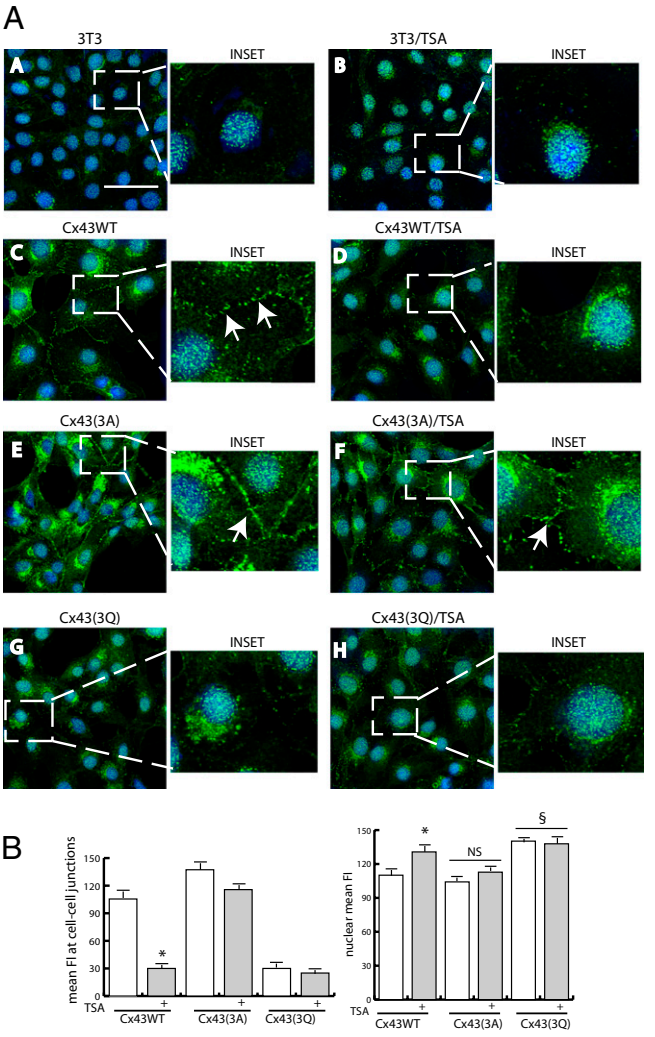

Fig. 4. Acetylation alters Cx43 intracellular distribution. (*A*) Confocal analysis of NIH 3T3 cells transient-transfected with mock (*A* and *B*), WT ($Cx43^{WT}$; *C* and *D*), or K → A ($Cx43^{3A}$; *E* and *F*) and K → Q ($Cx43^{3Q}$; *G* and *H*) connexin 43 expression vectors. Samples were analyzed before (*A*, *C*, *D*, and *G*) and after TSA treatment (*B*, *D*, *F*, and *H*). *Insets* show enlarged details representative of each experimental condition. Transfection efficiency was 80% on average for each vector. Experiments were repeated three times. (*B*) Quantitative evaluation of $Cx43^{WT}$, $Cx43^{3A}$, and $Cx43^{3Q}$ distribution at cell to cell junctions (*Left*) or the nuclear level (*Right*). Data are expressed as mean fluorescence intensity (MFI); about 300 cells were counted for each experimental condition. $*P < 0.05$ vs. $Cx43^{WT}$ in untreated cells; $^{§}P < 0.05$ vs. $Cx43^{WT}$ in untreated cells.

with PCAF and HDAC3, -4, and -5 and their functional interplay could be important in the regulation of Cx43 localization.

Discussion

This work provides evidence that, in dystrophic as well as normal hearts, Cx43 distribution in and out of ICDs may be regulated by the degree of N^{ε}-lysine acetylation, an observation that sheds light on this modification as a PTM other than phosphorylation or nitrosylation that is important for Cx43 association with its structurally and functionally relevant partners.

The cardiac alterations of DMD are triggered by dystrophin deficiency in humans and the mdx mouse strain, which is one of the classical models used to study their physiopathology. Although mdx mice disclose a mild phenotype compared with DMD and BMD patients, under appropriate stress conditions, they reproduce some of the most important electric impulse conduction

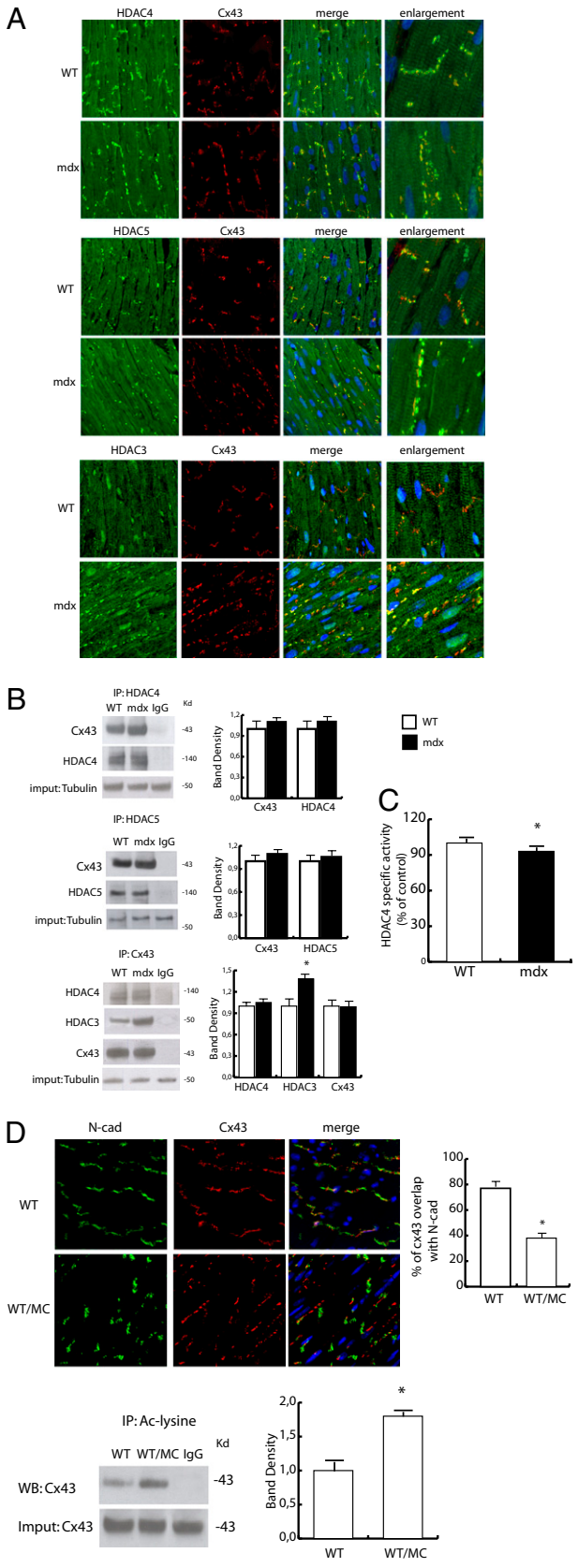

Fig. 5. HDACs localization, function, and association with Cx43. (*A*) Confocal analysis of Cx43 (red) and HDAC4 (green; *Top*), HDAC5 (green; *Middle*), or HDAC3 (green; *Bottom*) expression and distribution in the WT and mdx heart. Nuclei were counterstained with TOPRO3 (blue). (Scale bar, 50 μm.) Enlarged details are shown in the far right column. (Scale bar, 50 μm.) (*B*) Coimmunoprecipitation experiments showing HDAC4, -5, and -3 association with Cx43 in the WT and mdx heart. Relative densitometries are shown in *Right*. $*P < 0.05$. (*C*) HDAC4-specific activity evaluated in the WT and mdx heart samples. $*P < 0.05$. (*D*) Confocal analysis of *N*-cad (green) and Cx43 (red) expression and distribution in hearts from WT treated with MC1568 or equivalent amounts of solvent. Nuclei were counterstained with TOPRO3 (blue). (Scale bar, 50 μm.) The graph shows Cx43 and *N*-cad percentage of colocalization. $*P < 0.05$. *Lower* shows the acetylation level of Cx43 in WT treated with MC1568 or an equivalent amount of solvent (*Left*). Densitometry is shown to *Right*. $*P < 0.05$.

defects detectable in humans (18, 31). The production of reactive oxygen species (ROS) is one of the identified leading causes of protein and cellular membrane dysfunction associated with the disease (4). Interestingly, recent evidences indicated that the production of ROS also modulates the activity of epigenetic enzymes. Accordingly, we found that, in the heart of mdx mice, the total HAT activity was significantly increased and paralleled by a relatively high level of PCAF and p300 expression. This alteration was fully corrected by an antioxidant treatment, suggesting that the oxidative environment of the dystrophic cardiac muscle defines an important physiopathological condition upstream of the epigenetic alteration. Although other epigenetic enzymes could be involved in the control of Cx43, our current findings indicate HATs and HDACs as major regulatory players. Specifically, the evidence that Cx43 distribution and function may be regulated in mdx by N^{ε}-lysine acetylation in the presence of an altered HDAC/HAT balance and the possibility of reproducing this phenotype in normal mice exposed to proacetylation agents provide molecular insights about an unprecedented Cx43 control mechanism of epigenetic origin, which may account for at least some of the conduction defects seen in muscular dystrophy.

The identification of PCAF or HDAC3, -4, and -5 associated with Cx43 is another observation that, coupled with the presence of an acetylation-dependent alteration in Cx43 distribution and function, may provide directions for future development of innovative epigenetic drugs aimed at controlling cell to cell coupling, with potential consequences on cardiac function.

In this light, it is noteworthy that a HAT inhibitor, the anacardic acid, rescued Cx43 distribution in dystrophic hearts, opening the possibility of interventions aimed at ameliorating dystrophic cardiomyopathy through direct protein acetylation control. However, HDAC inhibitors, although certainly beneficial in the long-term treatment of mdx mice at least in part as consequence of their potent differentiation and antiinflammatory actions (8, 19, 32), rapidly determined Cx43 lateralization in normal mice. This evidence calls for further investigation of the efficacy and safety of HDAC inhibitors, with special attention to their effects on the cardiovascular system at least in the early stage of treatment.

In conclusion, the presence of ROS has been recently recognized as important for the regulation of Cx43 distribution and function in failing heart (9). Our work further expands this observation, suggesting the presence of a regulatory level that is upstream of Cx43 in the dystrophic heart: the activation of an oxidative-dependent protein acetylation pathway responsible for the N^{ε}-lysine acetylation of Cx43. Whether this or other epigenetically based mechanisms are involved in alterations associated with Cx43 in the failing heart or other heart diseases remains to be ascertained. Nevertheless, evidence is now accumulating about epigenetic processes meant for nonhistone protein modification that, transcending the limits of muscular dystrophy, could be considered as an additional control layer for fundamental cardiac functions such as contractility (27), cell to cell coupling, and electric impulse transmission.

CELL BIOLOGY

Methods

Animals and Treatments. All animals used in this work were 2-mo-old WT (strain C57/BlJ10) and syngeneic mdx mice purchased from Charles River. WT mice were injected i.p. daily for 4 d with histone deacetylase inhibitor SAHA (5 mg/kg, n = 7; ALEXIS-Biochemicals), class IIa-selective histone deacetylase inhibitor MC1568 (40 mg/kg; n = 6), or PCAF histone acetylase activator SPV106 (20 mg/kg; n = 7). Control animals were injected with saline solution and an equivalent amount of solvent (DMSO; n = 4). Mdx mice were injected i.p. daily for 4 d with the histone acetylase inhibitor ANAC (5 mg/kg, n = 6; ALEXIS-Biochemicals), the antioxidant NAC (200 mg/kg, n = 4), or saline solution with an equivalent amount of solvent (DMSO; n = 4; further details in *SI Methods*). The amounts of pentadecylidenemalonate 1b and ANAC used in the in vivo experiments were experimentally determined (Fig. S8).

HAT and HDAC Activity. HDAC (Upstate Biotechnology) and HAT (Biovision) fluorimetric assays were performed according to the manufacturer's instructions. Proteins were obtained from WT and mdx hearts homogenized in lysis buffer (20 mM Tris·HCl, pH 7.4, 150 mM NaCl, 5 mM EDTA, 1% Triton x-100, 10% glycerol supplemented with 1 mM PMSF and protease inhibitor mix); 100 μg total extract were used in each experiment.

Evaluation of HDAC4 Specific Activity. Assays were carried out as previously reported (33). Briefly, under liquid nitrogen, each tissue was pulverized to a powder with a mortar and pestle, and proteins were extracted with Lysis buffer (50 mM Tris·HCl, pH 7.0, 150 mM NaCl, 0.15% Nonidet P-40, 10% glycerol, 1.5 mM MgCl2, 1 mM $NaVO_4$, 1 mM NaF) with protease inhibitors (Sigma), 1 mM DTT, and 0.2 mM PMSF. Samples were incubated for 10 min on ice and centrifuged at 12,000 × g for 30 min at 4 °C; 250 μg total extract were used for each determination (details in *SI Methods*).

Confocal Analysis. Heart sections were deparaffinized, and confocal immunofluorescence analysis was performed according to a procedure previously described (8). Samples were analyzed using a Zeiss LSM510 Meta Confocal Microscope with 40× or 80× magnification. Laser power, beam splitters, filter settings, pinhole diameters, and scan mode were the same for all examined fields of each sample. Negative immunofluorescence control was performed using normal rabbit IgG instead of the rabbit primary antibody. The quantification of Cx43 present at the gap junction was evaluated measuring Cx43 and *N*-cad fluorescence intensities by Image J software. The Cx43 mean values obtained were then divided by *N*-cad mean values and expressed as percentages of overlap. For each sample, three independent fields were analyzed.

Statistical Analysis. Data represent the mean of at least three independent experiments ± SEM. The Student two-tailed t test was applied to calculate the statistic significance. A probability of less than 5% was considered significant ($P < 0.05$).

ACKNOWLEDGMENTS. This work was partially supported by Fondo per gli Investimenti della Ricerca di Base Grant RBLA035A4X-1-FIRB (to M.C.), Association Française Contre les Myopathies Grants DdT2-06 (to M.C.) and MNM2-06 (to C.G.), and Muscular Dystrophy Association Grant 88202 (to C.G.). C.C. is a PhD student of the School of "Scienze Endocrino-Metaboliche ed Endocrino-Chirurgiche" of the Chair of Endocrinology, Catholic University, Rome 00165, Italy.

1. Beggs AH (1997) Dystrophinopathy, the expanding phenotype. Dystrophin abnormalities in X-linked dilated cardiomyopathy. *Circulation* 95:2344–2347.
2. Bia BL, et al. (1999) Decreased myocardial nNOS, increased iNOS and abnormal ECGs in mouse models of Duchenne muscular dystrophy. *J Mol Cell Cardiol* 31:1857–1862.
3. Wehling-Henricks M, Jordan MC, Roos KP, Deng B, Tidball JG (2005) Cardiomyopathy in dystrophin-deficient hearts is prevented by expression of a neuronal nitric oxide synthase transgene in the myocardium. *Hum Mol Genet* 14:1921–1933.
4. Williams IA, Allen DG (2007) The role of reactive oxygen species in the hearts of dystrophin-deficient mdx mice. *Am J Physiol Heart Circ Physiol* 293:H1969–H1977.
5. Hitchler MJ, Domann FE (2007) An epigenetic perspective on the free radical theory of development. *Free Radic Biol Med* 43:1023–1036.
6. Illi B, et al. (2009) NO sparks off chromatin: Tales of a multifaceted epigenetic regulator. *Pharmacol Ther* 123:344–352.
7. Rahman I, Marwick J, Kirkham P (2004) Redox modulation of chromatin remodeling: Impact on histone acetylation and deacetylation, NF-kappaB and pro-inflammatory gene expression. *Biochem Pharmacol* 68:1255–1267.
8. Colussi C, et al. (2009) Nitric oxide deficiency determines global chromatin changes in Duchenne muscular dystrophy. *FASEB J* 23:2131–2141.
9. Smyth JW, et al. (2010) Limited forward trafficking of connexin 43 reduces cell-cell coupling in stressed human and mouse myocardium. *J Clin Invest* 120:266–279.
10. Tomaselli GF (2010) Oxidant stress derails the cardiac connexon connection. *J Clin Invest* 120:87–89.
11. Retamal MA, Cortés CJ, Reuss L, Bennett MV, Sáez JC (2006) S-nitrosylation and permeation through connexin 43 hemichannels in astrocytes: Induction by oxidant stress and reversal by reducing agents. *Proc Natl Acad Sci USA* 103:4475–4480.
12. Solan JL, Lampe PD (2005) Connexin phosphorylation as a regulatory event linked to gap junction channel assembly. *Biochim Biophys Acta* 1711:154–163.
13. Pahujaa M, Anikin M, Goldberg GS (2007) Phosphorylation of connexin43 induced by Src: Regulation of gap junctional communication between transformed cells. *Exp Cell Res* 313:4083–4090.
14. Severs NJ, Bruce AF, Dupont E, Rothery S (2008) Remodelling of gap junctions and connexin expression in diseased myocardium. *Cardiovasc Res* 80:9–19.
15. Dang X, Doble BW, Kardami E (2003) The carboxy-tail of connexin-43 localizes to the nucleus and inhibits cell growth. *Mol Cell Biochem* 242:35–38.
16. Colussi C, et al. (2010) Histone deacetylase inhibitors: Keeping momentum for neuromuscular and cardiovascular diseases treatment. *Pharmacol Res* 62:3–10.
17. Colussi C, et al. (2008) HDAC2 blockade by nitric oxide and histone deacetylase inhibitors reveals a common target in Duchenne muscular dystrophy treatment. *Proc Natl Acad Sci USA* 105:19183–19187.
18. Colussi C, et al. (2010) The histone deacetylase inhibitor suberoylanilide hydroxamic acid reduces cardiac arrhythmias in dystrophic mice. *Cardiovasc Res* 87:73–82.
19. Minetti GC, et al. (2006) Functional and morphological recovery of dystrophic muscles in mice treated with deacetylase inhibitors. *Nat Med* 12:1147–1150.
20. Whitehead NP, Pham C, Gervasio OL, Allen DG (2008) N-Acetylcysteine ameliorates skeletal muscle pathophysiology in mdx mice. *J Physiol* 586:2003–2014.
21. Balasubramanyam K, Swaminathan V, Ranganathan A, Kundu TK (2003) Small molecule modulators of histone acetyltransferase p300. *J Biol Chem* 278:19134–19140.
22. Choudhary C, et al. (2009) Lysine acetylation targets protein complexes and co-regulates major cellular functions. *Science* 325:834–840.
23. Giepmans BN (2004) Gap junctions and connexin-interacting proteins. *Cardiovasc Res* 62:233–245.
24. Hesketh GG, Van Eyk JE, Tomaselli GF (2009) Mechanisms of gap junction traffic in health and disease. *J Cardiovasc Pharmacol* 54:263–272.
25. Spange S, Wagner T, Heinzel T, Krämer OH (2009) Acetylation of non-histone proteins modulates cellular signalling at multiple levels. *Int J Biochem Cell Biol* 41:185–198.
26. di Bari MG, et al. (2006) c-Abl acetylation by histone acetyltransferases regulates its nuclear-cytoplasmic localization. *EMBO Rep* 7:727–733.
27. Gupta MP, Samant SA, Smith SH, Shroff SG (2008) HDAC4 and PCAF bind to cardiac sarcomeres and play a role in regulating myofilament contractile activity. *J Biol Chem* 283:10135–10146.
28. Sbardella G, et al. (2008) Identification of long chain alkylidenemalonates as novel small molecule modulators of histone acetyltransferases. *Bioorg Med Chem Lett* 18: 2788–2792.
29. Fischle W, Kiermer V, Dequiedt F, Verdin E (2001) The emerging role of class II histone deacetylases. *Biochem Cell Biol* 79:337–348.
30. Mai A, et al. (2005) Class II (IIa)-selective histone deacetylase inhibitors. 1. Synthesis and biological evaluation of novel (aryloxopropenyl)pyrrolyl hydroxyamides. *J Med Chem* 48:3344–3353.
31. Branco DM, et al. (2007) Cardiac electrophysiological characteristics of the mdx (5cv) mouse model of Duchenne muscular dystrophy. *J Interv Card Electrophysiol* 20:1–7.
32. Colussi C, et al. (2010) Proteomic profile of differentially expressed plasma proteins from dystrophic mice and following suberoylanilide hydroxamic acid treatment. *Proteomics Clin Appl* 4:71–83.
33. Nebbioso A, et al. (2009) Selective class II HDAC inhibitors impair myogenesis by modulating the stability and activity of HDAC-MEF2 complexes. *EMBO Rep* 10: 776–782.